This is a repository copy of *Accelerated carbonation testing of alkali-activated slag/metakaolin blended concretes: effect of exposure conditions*.

White Rose Research Online URL for this paper:
http://eprints.whiterose.ac.uk/97159/

Version: Accepted Version

1 **Accelerated carbonation testing of alkali-activated slag/metakaolin blended**

2 **concretes: effect of exposure conditions**

3

4 Susan A. Bernal,[1,2] John L. Provis,[2*] Ruby Mejía de Gutiérrez,[1] Jannie S.J. van Deventer[3,4]

5

6 [1]School of Materials Engineering, Composite Materials Group, CENM, Universidad del Valle, Cali,

7 Colombia

8 [2](current address) Department of Materials Science and Engineering, University of Sheffield, Sir

9 Robert Hadfield Building, Mappin St, Sheffield S1 3JD, United Kingdom

10 [3]Zeobond Pty Ltd, P.O. Box 210, Somerton, Victoria 3062, Australia

11 [4]Department of Chemical and Biomolecular Engineering, University of Melbourne, Victoria 3010,

12 Australia

13

14 * To whom correspondence should be addressed. Email j.provis@sheffield.ac.uk, phone +44 114

15 222 5490, fax +44 114 222 5943

16

17 **Abstract**

18 This paper addresses the effects of relative humidity and CO_2 concentration on the rate and effects of

19 accelerated carbonation in alkali-activated slag/metakaolin concretes. Strength and water absorption

20 are used alongside phenolphthalein measurements to monitor carbonation, and the effects of drying at

21 different relative humidities are particularly significant in controlling carbonation rates. Different

22 trends in the carbonation rate as a function of metakaolin content are observed when varying the CO_2

23 concentration, further revealing that the carbonation rates of these materials under accelerated

24 conditions are influenced strongly by the testing protocol. The standard phenolphthalein method for

25 testing carbonation depth appears only to be capturing the change in alkalinity with pore solution

26 carbonation, meaning that it does not correlate well with other performance parameters at high CO_2

27 concentrations.

28

29 **Keywords:** alkali-activated cement; concrete; granulated blast-furnace slag; carbonation; durability

30

31

32 **1. Introduction**

33

34 Durability of structures and structural concretes, particularly in the presence of aggressive agents, is a

35 topic of fundamental interest and importance in civil infrastructure and construction. Carbon dioxide

36   (CO_2) is particularly known to affect the durability of cement-based materials under long-term

37   exposure, through a degradation process referred to as carbonation [1-3]. This phenomenon is

38   controlled by both gas diffusion and chemical reaction mechanisms, and consequently its progress is

39   determined by both the chemistry of the binder and the permeability of the material. The effect of

40   carbonation in concrete structures is a reduction in the alkalinity of the material, leading to an

41   increased susceptibility to corrosion of embedded steel reinforcement, often accompanied by a

42   decrease in mechanical strength [2, 4, 5].

43

44   Carbonation of mortars and concretes produced using ordinary Portland cement has been widely

45   studied. In these systems, the CO_2 from the atmosphere diffuses through gas-filled pores and dissolves

46   in the pore solution to form aqueous HCO_3^-. This uptake of acidic CO_2 into the alkaline pore solution

47   reduces the internal pH of the binder, and the dissolved carbonate also reacts with the calcium-rich

48   hydration products present in the matrix, mainly with the portlandite $(Ca(OH)_2)$, calcium silicate

49   hydrate (C-S-H) and calcium aluminate hydrate phases, to form solid calcium carbonates [4, 6, 7]. In

50   Portland cement-based systems, it is well known that the progress of carbonation is dependent on the

51   chemical nature of the binder phases with which the CO_2 is going to react, as well as the factors

52   determining the diffusion rate of the gaseous CO_2, such as the pore network and exposure

53   environment, in particular relative humidity [8-11]. It has been reported [9] that carbonation is more

54   rapid at intermediate relative humidity (50–70%), and this is attributed to interactions between drying

55   and carbonation processes [12], as the presence of a very high fraction of pores filled with water

56   hinders the diffusion of CO_2, while sufficient water is required to promote the solvation and hydration

57   of the carbon dioxide. Under intermediate moisture conditions both reaction kinetics and diffusion of

58   CO_2 are favoured, which leads to acceleration of the carbonation process [4].

59

60   In the case of concretes based on alkali-activated binders, there is limited existing knowledge about

61   the long-term in-service stability of these materials, although the studies that have been published

62   show generally moderate to low carbonation rates (<0.5 mm/yr), similar to the carbonation rate of

63   Portland cement concretes, under service conditions in continental climates [13-15]. Shi, Krivenko

64   and Roy report the natural carbonation rates of concrete structures with ages between 12 and 40 years,

65   located in Russia, Ukraine and Poland [14]. The concretes were produced from alkali-activated slag,

66   using alkaline activator solutions of sodium metasilicate, sodium carbonate and potassium carbonate,

67   and had 28-day compressive strengths between 35 - 82 MPa. The in-service carbonation rates,

68   measured using the phenolphthalein method, did not exceed 1 mm/year in any of the cases described.

69   Similar results were identified in 7-year-old silicate-activated slag concretes [16], where the

70   carbonated depths identified were much lower than would be predicted through calculations based on

71 accelerated carbonation testing, demonstrating that the exposure conditions used in accelerated testing

72 do not replicate the phenomena that take place under natural service conditions.

73

74 On the other hand, laboratory studies of pastes and mortars of alkali-activated slag, and

75 slag/metakaolin blends [15, 17-21], have indicated high susceptibility to carbonation in these

76 materials under accelerated conditions, compared with conventional cements. It is proposed that this

77 is due particularly to effects related to pore solution alkalinity [22] and binder chemistry, especially

78 the absence of portlandite as a reaction product in these binders. More recently it has been identified

79 [23] that drying of alkali-activated materials induces changes in their microstructure. This causes

80 severe microcracking, which is deleterious when pre-conditioning specimens prior to analysis of

81 water absorption properties and accelerated carbonation testing. Considering these observations, it is

82 evident that there is the need to develop a better understanding of the real meaning of the results

83 obtained in alkali-activated materials, and how accelerated carbonation tests should be conducted, as

84 the divergences between accelerated and natural carbonation rates of alkali-activated concretes are

85 remarkable [16].

86

87 The carbonation of concrete under ambient conditions is generally relatively slow, as a consequence

88 of the relatively low concentration of CO_2 in the atmosphere (0.03 – 0.04%). This has led to the

89 development of experimental methods based on accelerated carbonation under controlled conditions,

90 through exposure to high CO_2 concentrations for shorter periods of time. It has been noted [24] that a

91 short period of accelerated carbonation in Portland cement-based materials is not necessarily directly

92 analogous to long term exposure to natural atmosphere, which involves differences in moisture

93 distribution under different drying periods, and gradual changes in the micropore structure due to

94 ageing and carbonation. A proposed European standard method [25] for testing the susceptibility of

95 Portland cement-based materials to carbonation has been discussed in detail by Harrison et al. [26],

96 and adopted recently by some nations, but not in general across the EU [26]. Some limitations of

97 common accelerated test methods, such as repeatability and reproducibility, have also been identified,

98 even in application to Portland cement-based systems [27, 28].

99

100 For the specific case of alkali-activated binders, recent results [22] reveal that the mechanism of

101 carbonation in alkali activated slag which is induced using accelerated test methods is strongly

102 affected by the CO_2 concentration, leading to differences in the chemistry of the alkali carbonate

103 phases formed as a result of carbonation, and also the pH and carbonate/bicarbonate ratio of the

104 remaining pore solution. This will therefore change both the CO_2 uptake rate and the influence of the

105 carbonated pore solution on steel corrosion chemistry, meaning that the test results must be carefully

106 interpreted in order to give an accurate prediction of either the rate or the effects of carbonation in

107 these materials under natural conditions. In particular, it appears from thermodynamic calculations

108 related to pore solution chemistry [22] that accelerated testing will overestimate both the rate and

109 degradation effects of carbonation in alkali-activated binders. From these results, it seems likely that

110 if an alkali-activated concrete and a Portland cement concrete show the same carbonation depth in an

111 accelerated test, the alkali-activated material will suffer less carbonation under natural conditions, and

112 thus the service life would be much higher. However, further detailed experimental work related to

113 understanding the effects induced by different accelerated testing conditions is undoubtedly required

114 before such statements can be fully validated.

115

116 This indicates that the exposure conditions which are used to induce accelerated carbonation of alkali-

117 activated materials need to be studied, in order to provide recommendations for appropriate testing

118 protocols, and also to aid in interpretation of the results obtained. The aim of this study is therefore to

119 assess the effects of relative humidity and CO_2 concentration on the carbonation rate of alkali-

120 activated concretes during accelerated testing. The concretes tested have a binder based on a

121 combination of granulated blast furnace slag (GBFS) and metakaolin (MK), activated by sodium

122 silicate solutions, where the addition of the metakaolin serves to regulate the setting of these materials

123 which are based on an otherwise very rapidly-reacting slag, and also enhances strength when the

124 activator dose is sufficient [29, 30]. In addition to carbonation depth measurements, variations in

125 mechanical strength and pore network properties, investigated in an indirect way via water absorption

126 tests, are monitored during CO_2 exposure, to obtain a deeper understanding of the microstructural

127 changes in the concretes which are induced under different exposure conditions.

128

129

130

131 **2. Materials and methods**

132

133 **2.1. Materials**

134

135 The primary raw material used in this study was a Colombian granulated blast furnace slag (GBFS)

136 from the factory Acerías Paz del Río. Its specific gravity was 2900 kg/m^3 and Blaine fineness was 399

137 m^2/kg. The particle size range, determined through laser granulometry, was 0.1–74 μm, with a d_{50} of

138 15 μm. The metakaolin (MK) used was generated in the laboratory by calcination of a kaolin

139 containing minor quartz and dickite impurities [29]. Calcination was carried out at 700°C in an air

140 atmosphere, for 2 h. The particle size range of the MK was 1.8–100 μm, with a d_{50} of 13.2 μm and

141 10% of particles finer than 4 μm.

142

143 **Table 1.** Compositions of the MK and GBFS used, from X-ray fluorescence analysis. LOI is loss on
144 ignition at 1000°C

Raw material	Component (mass % as oxide)							
	SiO_2	Al_2O_3	CaO	Fe_2O_3	MgO	TiO_2	Others	LOI
GBFS	32.29	16.25	42.45	2.35	2.87	0.50	0.57	2.72
MK	50.72	44.63	2.69	-	-	-	0.94	1.02

146 Alkaline activating solutions were formulated by blending a commercial sodium silicate solution
147 (32.4 wt.% SiO_2, 13.5 wt.% Na_2O and 54.1 wt.% H_2O), and 50 wt.% NaOH solution, with the slag
148 and metakaolin, to reach the desired overall molar ratios (specified as SiO_2/Al_2O_3 (S/A)), and
149 corresponding to a concentration of activation of 11-12% Na_2O relative to the amount of binder (i.e.,
150 11-12 g Na_2O per 100 g GBFS+MK).

151

152 Crushed gravel and river sand were used as coarse and fine aggregates. The coarse aggregate was of
153 19 mm maximum size, with a specific gravity of 2790 kg/m^3 and absorption of 1.23%. The specific
154 gravity, absorption, and fineness modulus of the sand were 2450 kg/m^3, 3.75% and 2.57, respectively.

155

156 **2.2. Concrete mixes**

157

158 The concretes were produced with total binder (GBFS+MK) contents of 400 kg/m^3 and a total
159 water/(GBFS+MK+anhydrous activator) ratio of 0.47. Fresh concrete was mixed, poured into
160 cylindrical steel moulds (ϕ = 76.2 mm, h = 152.4 mm), tamped and levelled. The concrete specimens
161 were then cured in a humidity-controlled chamber at 25±5°C and 90% relative humidity (RH), for 28
162 days, with the moulds removed after 24 hours. The mix designs are given in Table 2. Detailed
163 analysis of the evolution of engineering (compressive and flexural strength) and durability properties
164 (water absorption properties, chloride permeability and carbonation) of the concrete mixes assessed in
165 this study as a function of the time of curing is reported in [30].

166

167 **Table 2.** Mix designs of the concretes. All quantities are in kg/m^3 of fresh concrete

Component	GBFS/(GBFS+MK)		
	1.0	0.9	0.8
GBFS	400	360	320
MK	-	40	80
Sodium silicate solution	120	136	132
NaOH (50 wt.% solution)	68	72	78
Coarse aggregate	832	816	808
Sand	832	816	808
Free water	132	124	124
Overall SiO_2/Al_2O_3 molar ratio	4.4	4.0	3.6
Activator concentration	10.6	11.6	12.0

5

(% Na$_2$O by mass of GBFS + MK)

168

169

2.3. Accelerated carbonation testing

171

After 28 days of curing the specimens were removed from the humidity chamber, and then the top ends of the specimens were covered using an acrylic resin (Acronal ®), applying a minimum of 4 layers, to direct the ingress of CO_2 through the curved face of the cylinders during testing. Samples were then transferred to the carbonation chamber for CO_2 exposure, without application of an intermediate drying or conditioning step. This was done to minimise any potential microcracking or differences in sample maturity which would be observed if they were conditioned for extended periods at the testing relative humidity, a step which is specified in many testing protocols for Portland cement systems.

180

2.3.1. Variation of relative humidity

182

An accelerated carbonation testing system with automated control of temperature, humidity and CO_2 concentration was used to induce the carbonation of concrete specimens. A CO_2 concentration of 1.0 ± 0.2%, was used, at a temperature of 25 ± 2 °C, and RH values of 50 ± 5%, 65 ± 5%, and 80 ± 5%, where the uncertainties quoted here are the maximum allowable deviations from setpoints as specified by the supplier of the chamber control systems. Specimens were removed from the chamber after 250 or 500 h of exposure, and the depth of carbonation was measured by treating the surface of a freshly cleaved specimen with a 1% solution of phenolphthalein in alcohol. In the uncarbonated part of the specimen, where the concrete was still highly alkaline, purple-red colouration was obtained, while there was no colour change observed in the carbonated region. Each result is reported as the average depth of carbonation measured at eight points, using two replicate samples (four points per sample; the standard deviation of each carbonation depth measurement is similar to or smaller than the size of the points on the graphs as plotted). The properties of uncarbonated samples after 28 days of curing are used as reference values, indicated as zero hours of exposure.

196

2.3.2. Variation of CO_2 exposure concentration

198

Specimens were exposed to CO_2 concentrations of 1 ± 0.2% and 3.0 ± 0.2%, at a relative humidity of 65 ± 5%. After 250, 500, 750 and 1000 h of exposure, carbonation depths were determined as described above.

202

6

203   **2.4. Testing protocols**

204

205   Carbonated and uncarbonated concretes were tested for compressive strength following the standard

206   procedure ASTM C39/C39M-09a (Standard Test Method for Compressive Strength of Cylindrical

207   Concrete Specimens). Total porosity and absorption were determined before and after carbonation

208   according to the standard procedure ASTM C642-06 (Standard Test Method for Density, Absorption,

209   and Voids in Hardened Concrete), where the samples are dried and then boiled in water to determine

210   the total volume of permeable voids. Capillary sorptivity was assessed by applying the standard

211   procedure EMPA–SIA 162/1 [31], in which water is allowed to pass from a damp sponge into a dried

212   cylindrical sample through a process of capillary suction, and the mass of the sample is monitored as a

213   function of time.

214

215   **3. Results and discussion**

216

217   **3.1.   Effect of relative humidity on the accelerated carbonation of alkali-activated GBFS/MK**

218   **blends**

219

220   3.1.1.   Carbonation rate

221

222   Figure 1 shows the carbonation depth as a function of time and relative humidity for the samples

223   containing different percentages of metakaolin. There are two clearly distinct types of behaviour

224   shown by the samples when considering carbonation as a function of time:

225   -   All of the GBFS-only samples, and the sample with GBFS/(GBFS+MK) = 0.9 exposed at 80%

226   RH, show relatively slow initial carbonation, but then the ingress of the carbonation front

227   accelerates, and the increment in carbonation depth from 250-500 h is more than the carbonation

228   observed in the first 250 h

229   -   All of the samples with GBFS/(GBFS+MK) = 0.8, and the samples with GBFS/(GBFS+MK) = 0.9

230   exposed at 50 and 65% RH, show a deceleration in carbonation with time, with more carbonation

231   in the first 250 h than in the subsequent 250 h.
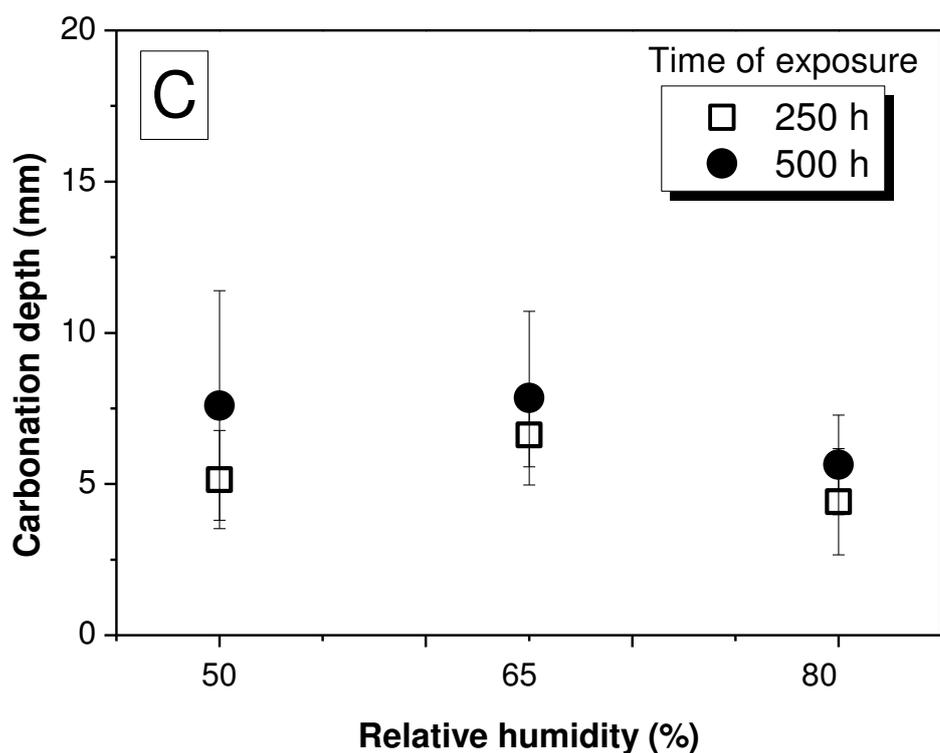
232

233
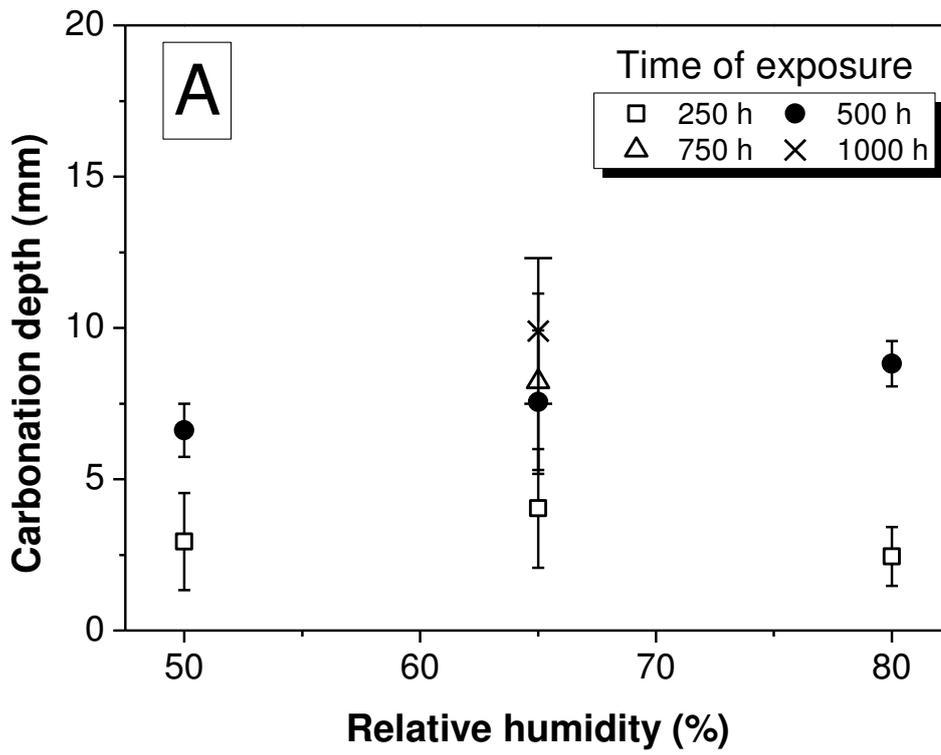
234
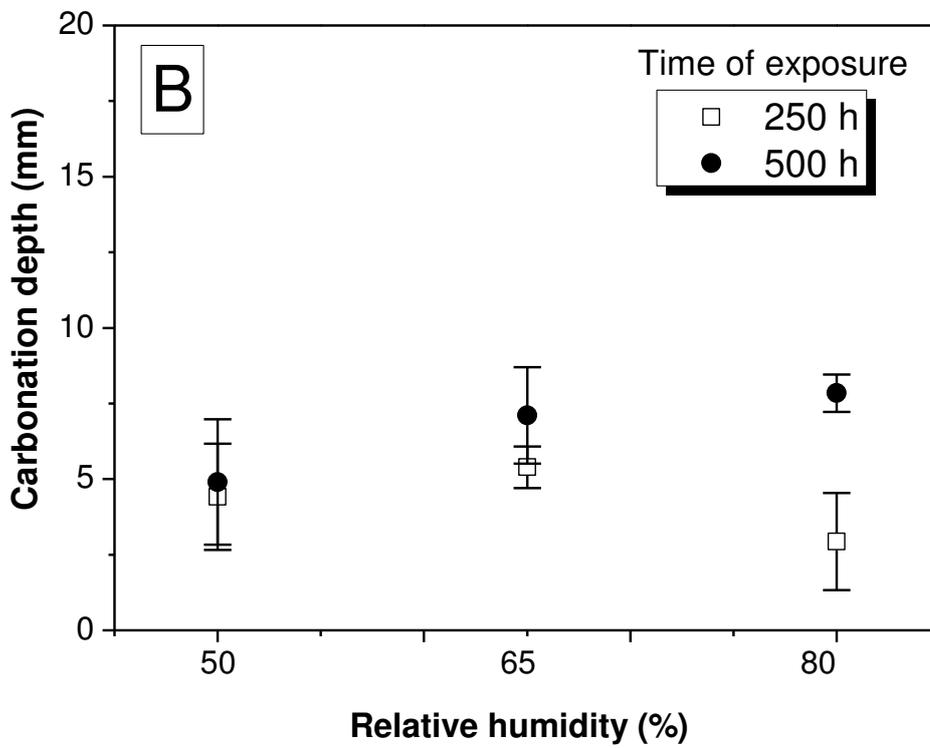
235

236

237   **Figure 1.** Carbonation depth as a function of the relative humidity and time of exposure in alkali-

238   activated GBFS/MK concretes, formulated with GBFS/(GBFS+MK) ratios of (A) 1.0, (B) 0.9 and (C)

239   0.8, at 1% CO_2. Error bars show ± 1 standard deviation among 5 measurements per sample.

240

241   Figure 1 also shows differences in the trend in carbonation depth as a function of relative humidity,

242   depending on the binder composition and the exposure time. In specimens solely based on GBFS

243   (Figure 1A) similar carbonation depths are identified at each different RH during the first 250 h of

244   exposure, and the carbonation depth increases with RH after 500 h of CO_2 exposure. A similar trend is

245   observed in specimens with GBFS/(GBFS+MK) = 0.9, although the carbonation rate within the first

246   250 h at 80% RH is notably lower than at the other relative humidities studied. Similar results are

247   observed at higher content of MK in the binder (GBFS/(GBFS+MK) = 0.8, Figure 1C) with the most

248   rapid carbonation observed at intermediate humidity.

249

250   The acceleration in carbonation of some of the concretes (Figure 1A,B) between the first 250 h and

251   the subsequent 250 h of curing is to some extent counterintuitive; such a change in kinetics would not

252   be expected if the process were simply controlled by either diffusion or chemical reaction

253   mechanisms [32, 33]. Even if the microstructural damage associated with the carbonation-induced

254   decalcification of the C-A-S-H gel to form calcium carbonate products [17] was so severe that the

255   damaged material did not provide any barrier to CO_2 diffusion, this would result in a linear rate of

9

256 carbonation, but could not explain an acceleration in rate. There must therefore be a combination of
257 drying and carbonation effects which leads to this apparent acceleration during this timeframe. There
258 is only one dataset available (Figure 1A) which contains data at 750 and 1000 h for a sample which
259 showed an acceleration effect; these data show that the carbonation decelerated again after 500 h,
260 which is consistent with the development of some extent of diffusional resistance to mass transport in
261 the later stages of carbonation, as would be expected from the thickness of the carbonated layers on
262 the samples.

263

264 The higher final extent of carbonation at higher relative humidities is consistent with the trends
265 reported for Portland cement concretes containing supplementary cementitious materials [34, 35],
266 where it is expected that the presence of water-saturated pores will hinder the diffusion of CO_2
267 through the material. Partially water-filled pores are known to accelerate carbonation through
268 convective mass transport, and also by providing high interfacial areas for transfer of CO_2 from gas to
269 liquid (and thus subsequently to solid) phases [9, 11]. For the GBFS-only samples, which have the
270 lowest water absorption in the uncarbonated state [30], and for the GBFS/(GBFS+MK) = 0.9 sample
271 at high (80%) relative humidity, it is likely that the pores are more extensively filled with water, so
272 the start of carbonation is slowed after the drying front has begun to enter the sample. The higher
273 water absorption measured for the uncarbonated GBFS/(GBFS+MK) = 0.8 samples [30] indicates that
274 there are already unsaturated pores within the concrete prior to the start of the carbonation tests for
275 these concretes, and the observed carbonation behaviour does not show an acceleration event.

276

277 Comparing the samples with different MK contents, it appears that when concretes are exposed under
278 comparable relative humidity conditions for 500 h, increased metakaolin content will usually give a
279 lower extent of carbonation. The only exception to this trend in Figure 1 is the sample with
280 GBFS/(GBFS+MK) = 0.8 at 50% RH, which is more rapidly carbonated than the sample with
281 GBFS/(GBFS+MK) = 0.9 under the same conditions. It is likely that this is related to the higher
282 porosity of the concretes with GBFS/(GBFS+MK) = 0.8 [30], as will be discussed in detail below.

283

284   3.1.2.   Residual compressive strength

285

286 The residual compressive strength (Figure 2) represents the ratio of the strengths of the concretes
287 before and after exposure to CO_2, providing a direct means of comparison of the samples which had
288 different strengths before carbonation (GBFS/(GBFS+MK) = 1.0: 63 MPa; GBFS/(GBFS+MK) = 0.9:
289 73 MPa; and GBFS/(GBFS+MK) = 0.8: 53 MPa). Concretes based solely on GBFS (Figure 2A) and
290 with GBFS/(GBFS+MK) = 0.9 (Figure 2B) show, over the first 250 h of exposure, only slight
291 reductions in the compressive strength relative to the uncarbonated concretes at relative humidities of

292   65% and 80%, while specimens exposed at an RH of 50% exhibit a reduction in the compressive
293   strength of around 15%. Similar trends are visible for specimens exposed for longer periods of time
294   (500 h), although the extent of strength loss increases notably with time. The effect of RH on the
295   carbonation progress of the concretes assessed seems to be more significant with the inclusion of MK
296   in the binder.
297
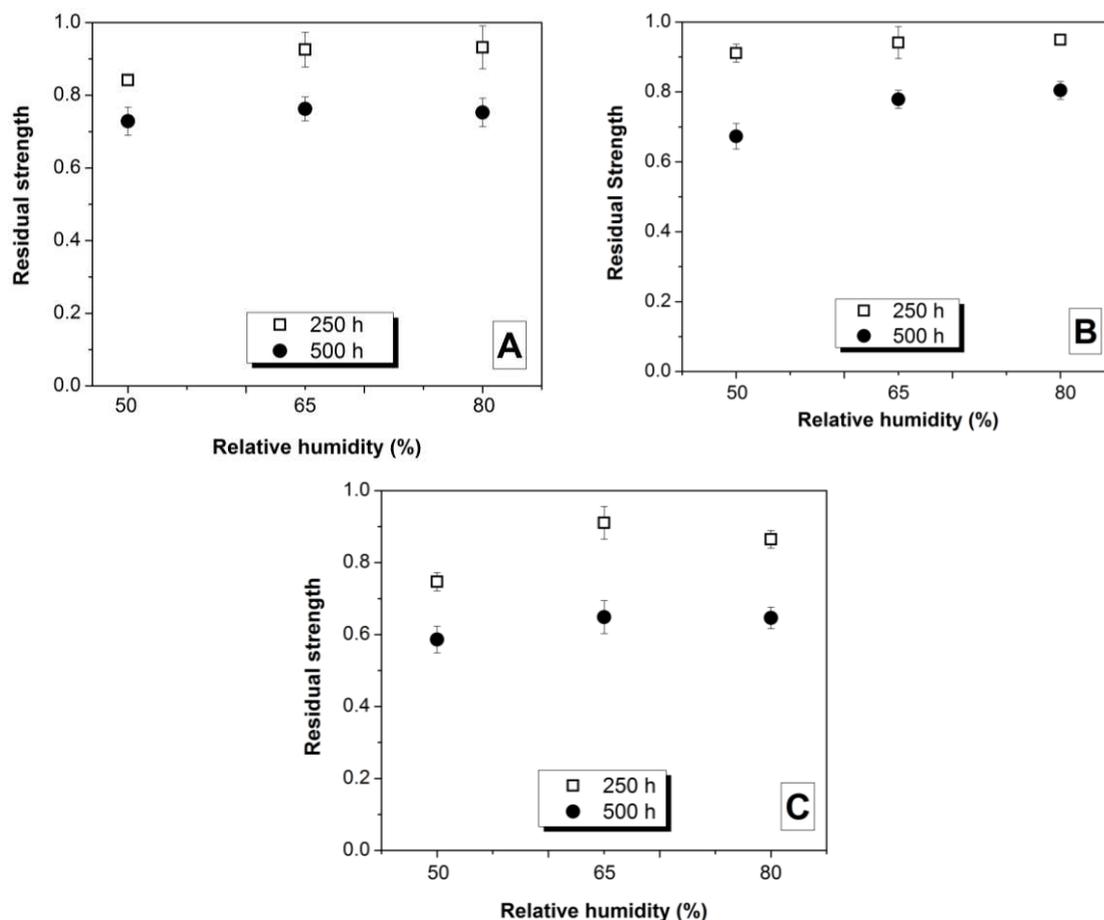
298   **Figure 2**. Residual compressive strengths of partially accelerated-carbonated concretes based on
299   alkali-activated slag/metakaolin blends formulated with GBFS/(GBFS+MK) ratios of (A) 1.0, (B) 0.9
300   and (C) 0.8, as a function of the relative humidity, at 1% CO_2. Error bars correspond to one standard
301   deviation of three measurements.
302

303   In a previous study where carbonation of some of these mix designs was studied at a single RH (65%)
304   for up to 1000 h [30], the correlation between carbonation depth and residual strength was observed to
305   be approximately linear for the concretes containing no more than 10% MK (GBFS/(GBFS+MK) ≥
306   0.9). However, such a relationship is not evident across the different RH values when comparing
307   Figures 1 and 2, particularly for the samples containing MK. The samples with GBFS/(GBFS+MK) =
308   0.9 exposed at 50% RH showed almost no additional carbonation depth (Figure 1B), but a marked
309   loss of strength (Figure 2B), between 250-500 h of exposure. The same mix exposed at 80% RH

11

310   showed a relatively rapid progression of the carbonation front, but almost no change in compressive
311   strength, between 250-500 h. However, the main disagreement between the carbonation depth and
312   carbonation rate data is visible when comparing the influence of RH on these two parameters: in each
313   case, 65% RH leads to the highest carbonation depth after 250 h of exposure, but the highest residual
314   strength after the same exposure time. The samples with GBFS/(GBFS+MK) = 0.8 are most deeply
315   carbonated, and lose the most strength, after 500h at 50% RH, but agreement between the conditions
316   which cause the greatest extent of damage as determined by these two different measures is not
317   observed for the concretes with GBFS/(GBFS+MK) = 0.9 or 1.0.

318
319   3.1.3.   Total porosity and absorption
320

321   The carbonation of alkali-activated concretes leads to an increase in the volume of permeable pores
322   (Figure 3) so that the volume of permeable voids of carbonated specimens is twice the porosity of
323   uncarbonated samples, when the porosity of the sample as a whole is measured; considering the fact
324   that there is an undamaged core in most of the cylinders tested, this change may even be more notable
325   if solely the carbonated part of the sample were to be considered. This increase in porosity is in
326   general slightly greater when carbonation is carried out at increased relative humidities, but the
327   differences between different RH values are not highly significant.

328
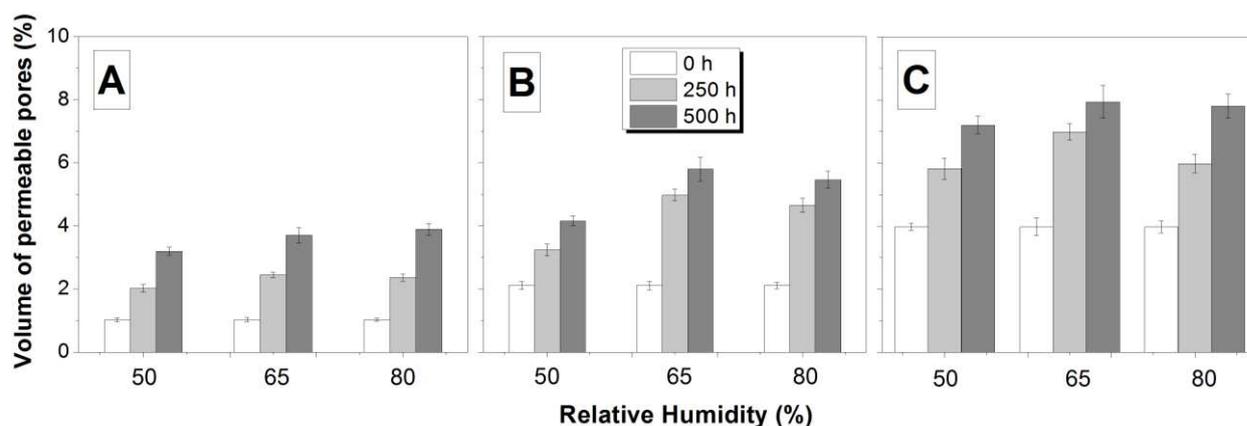
330   **Figure 3**. Porosity of partially carbonated concretes based on alkali-activated slag/metakaolin blends
331   formulated with GBFS/(GBFS+MK) ratios of (A) 1.0, (B) 0.9 and (C) 0.8, as a function of the relative
332   humidity, at 1% CO_2. Error bars correspond to one standard deviation of four measurements

333

334   Increased porosity is exhibited by concretes exposed to CO_2 over longer times, as expected with
335   reference to the progress of the carbonation reaction in the material. Mixes with GBFS/(GBFS+MK)
336   = 0.8 show the highest total porosity of the specimens studied, which might contribute to the higher
337   carbonation rate identified in these concretes after 250 h of exposure compared with the systems

338   including lower contents of MK. In this case, the samples exposed at 65% RH show the largest
339   increment in total porosity after 250 h of exposure; however, comparable porosities can be observed
340   after 500 h when the exposure to CO_2 is conducted at 65% or 80% RH.
341
342   These results agree reasonably well with the trends in carbonation depth as a function of relative
343   humidity (Figure 1C), but disagree with the residual compressive strength data obtained for these
344   specimens, where the lowest residual strengths were reported when the exposure was conducted at
345   50% RH (Figure 2C). It is thus suggested that the different protocols for assessing the progress and
346   influence of carbonation on an alkali-activated concrete are influenced in different ways by the
347   relative humidity conditions under which the test is conducted, and this is likely to be very important
348   when comparing data across different investigations, where various parameters are assessed under
349   different conditions. This means that different trends will be obtained, depending on which
350   performance parameters are selected for analysis.
351
352   Total water absorption values for the concretes assessed are shown in Table 2, and it can be seen that
353   although the influence of exposure RH on water absorption (as measured by the ASTM C642 test) is
354   relatively minor, higher absorptions are generally observed in concretes with MK in the binder when
355   exposed to carbonation at 65% RH, especially at longer times of exposure. It has been reported that,
356   for conventional Portland cement-based concretes [36], absorption values of 3% and total porosity
357   values of 10% are able to be related to concretes with good durability. Based on this, it is possible to
358   suggest that all the concretes assessed here, both before and after CO_2 exposure, have the potential to
359   be highly durable.
360
361   **Table 2.** Water absorption (wt.%) of concretes based on alkali-activated GBFS/MK blends exposed to
362   CO_2 under different relative humidities

GBFS/(GBFS+MK)	Relative humidity (%)	Time of exposure to CO_2 (hours)		
		0	250	500
1.0	50		1.27	1.53
	65	0.28	0.99	1.27
	80		1.20	1.32
0.9	50		2.09	2.15
	65	0.58	2.16	2.29
	80		2.10	2.30
0.8	50		2.68	2.98
	65	1.38	2.95	3.11
	80		2.73	2.99

363
364

13

365   As CO_2 can diffuse through both large and capillary pores, the total porosity is not the only factor that

366   can determine the progress of carbonation in alkali-activated concretes. For the mixes assessed here, it

367   has been observed when applying the standard procedure EMPA – SIA 162/1 [31] to study the

368   capillary uptake of water into a dried sample, that before carbonation the concretes present similar

369   resistance to water penetration ($\sim 1 \times 10^7$ s/m^2) [30]. This parameter is one of the main coefficients

370   describing the capillary sorptivity of these materials, and provides information regarding the geometry

371   of the pore network of the assessed samples, where a higher resistance to water penetration indicates a

372   more tortuous pore structure hindering mass transport through the material. The fact that similar

373   values of resistance to water penetration are obtained across the concrete mixes studied indicates that

374   these materials present approximately comparable pore structures. Consequently, the differences in

375   the rates of carbonation at early stages of reaction of the mixes assessed are more likely to be

376   associated with the carbonation starting in the capillary pores, increasing the pore size (as previously

377   identified in alkali-activated mortars [9-10]), and thus diminishing the effect of the different quantities

378   of water present at different RH values.

379

380   **3.2. Effect of the CO_2 concentration on the carbonation of concretes based on activated**

381   **GBFS/MK blends**

382

383   Results reported in a previous study [22] show that accelerated carbonation induced in the pore

384   solutions of alkali-activated binders under different CO_2 concentrations promotes the formation of

385   different carbonation products, depending on both the CO_2 concentration and the temperature of the

386   test. This indicates that increased partial pressures of CO_2 shift the reaction equilibrium expected

387   under natural carbonation conditions, and therefore promote mechanisms which may lead to

388   disproportionately faster degradation of the material compared to what is likely to occur in actual

389   service. Thus, conflicting results could be obtained if the carbonation progress in alkali-activated

390   concretes is tested under different CO_2 exposure conditions, and this issue is examined in detail in the

391   following section. All the tests described in this section are conducted at 65% RH.

392

393   3.2.1. Carbonation rate

394

395   As discussed in detail in section 3.1 above, concretes exposed to 1% CO_2 (Figure 4A) show a higher

396   carbonation extent at increased contents of MK in the binder; however, the difference between

397   GBFS/(GBFS+MK) ratios of 0.8 and 0.9 is in general minor, while there is a notable difference

398   between the concretes with and without MK. Increasing the CO_2 concentration to 3% (Figure 4B)

399   promotes much faster carbonation of the specimens, as expected. However, its effect is more

400   detrimental in the concretes with GBFS/(GBFS+MK) = 0.8 than with GBFS/(GBFS+MK) = 0.9 or

14

401   1.0. This indicates that 3% CO_2 is too high a concentration of CO_2 to enable reliable prediction of the

402   in-service carbonation performance of alkali-activated concretes with different binder mix designs, as

403   it may not be possible to distinguish which differences are due to actual better or worse carbonation

404   resistance of the samples, and which are due to differences in the aggressiveness of the test towards

405   different binder chemistries. This is an important point, and further discussion is required to determine

406   the reasons for this behaviour.

407
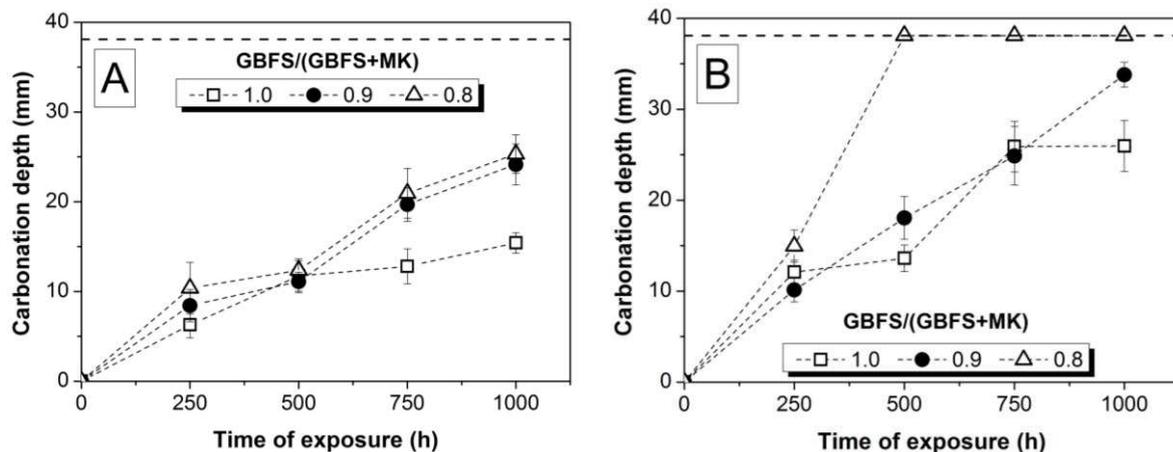
408

409   **Figure 4.** Accelerated carbonation progress of alkali-activated slag/metakaolin blended concretes

410   induced at (A) 1% CO_2 and (B) 3% CO_2, and 65% RH. The horizontal dashed line in each plot

411   represents full carbonation of the cylindrical specimens used in the tests. Each value is the average of

412   20 measurements taken from two specimens. Error bars correspond to one standard deviation.

413

414   After 250 h of exposure, the concretes with GBFS/(GBFS+MK) = 0.8 show the highest carbonation

415   depths, consistent with the greater volume of permeable pores determined in these specimens before

416   testing, when compared with the concretes with GBFS/(GBFS+MK) = 0.9 or 1.0. At longer times of

417   exposure, the carbonation rates of concretes with GBFS/(GBFS+MK) = 0.9 or 1.0 remain comparable

418   when exposed to 3% CO_2 (Figure 4B), although there was a notable difference between these

419   specimens at 1% CO_2 (Figure 4A). When including 20% MK in the binder (GBFS/(GBFS+MK) =

420   0.8) and exposing the material to 3% CO_2, the carbonation progresses so rapidly that the concrete

421   specimens tested here (38.1 mm radius cylinders) are completely carbonated after only 500 h of

422   exposure.

423

424   This, combined with the porosity data in Figure 3 and in reference [30], indicates that concretes

425   presenting a higher volume of permeable pores before testing will be more aggressively subject to

426   carbonation penetration at higher CO_2 concentrations than would be expected when the material is

427   exposed to more moderate CO_2 concentrations. It is noted that 3% CO_2 is actually not a particularly

428 high concentration for use in an accelerated carbonation test for Portland cement systems.
429 Concentrations far exceeding this value (and even up to 100%) are widely used in international testing
430 programs for Portland cement concretes [28], although there has been limited systematic study of the
431 influence of these parameters on the chemistry of non-traditional cements and concretes [37]. This
432 strong dependence on CO_2 concentration when comparing binder types may also provide misleading
433 conclusions about the 'real' quality of the material in service, considering that alkali-activated
434 concretes often exhibit a substantial reduction in permeability at advanced ages of curing, and
435 therefore will behave differently if they are assessed at more mature ages [30].
436
437

438   3.2.2.   Residual mechanical strength
439

440 Residual mechanical strengths of specimens carbonated under 1% and 3% CO_2 environments are
441 shown in Figure 5. These results show that decreases in the compressive strength are induced as
442 consequence of the carbonation of the specimens, and that this is not strongly dependent on the
443 concentration of CO_2 exposure. The concretes including MK as a secondary binder component show
444 very little effect of CO_2 concentration on residual strength, while the slag-only binders show slightly
445 more loss of strength at 3% CO_2 than at 1%. However, although some samples revealed complete
446 carbonation when determined using the phenolphthalein indicator (Figure 4B; samples with
447 GBFS/(GBFS+MK) = 0.8 at 3% CO_2), the remnant compressive strength of those concretes (Figure
448 5B) is comparable with what is obtained in specimens of the same mix design carbonated at 1% CO_2
449 (Figure 5A), where these specimens showed only partial carbonation when carbonation depth was
450 determined using the same methodology.
451
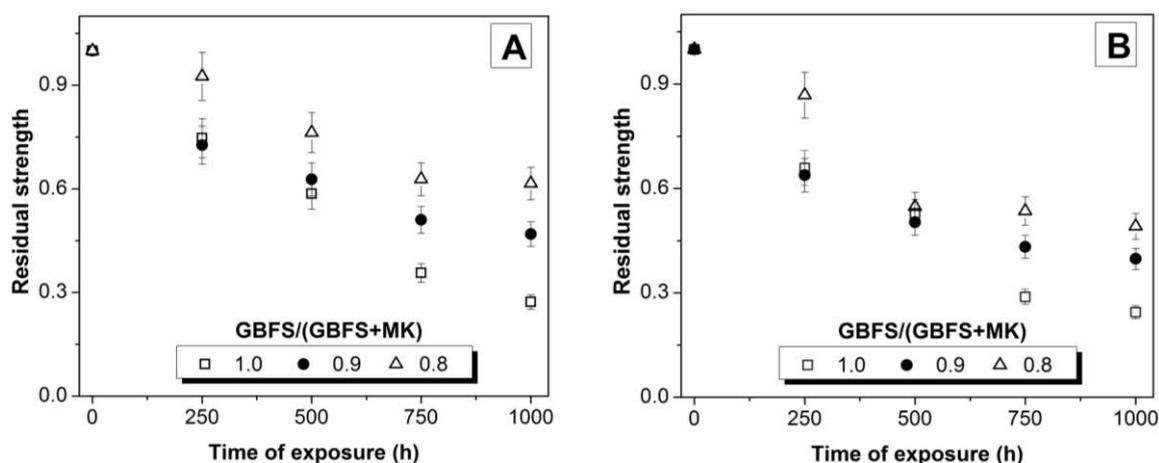
453 **Figure 5.** Effect of the CO_2 concentration of exposure on the residual compressive strength of
454   partially carbonated concretes based on alkali-activated slag/metakaolin blends, exposed to

16

455   carbonation at (A) 1% or (B) 3% CO_2, and 65% RH. Error bars correspond to one standard deviation

456   of three measurements.

457

458   It therefore becomes evident that there is not a direct correlation between the degree of ingress of the

459   carbonation front, as identified using the phenolphthalein indicator, and the degree of degradation of

460   the material as measured by residual mechanical strength. If complete carbonation of the matrix was

461   taking place in these systems, the loss of loading capacity should be approximately proportional to the

462   loss of undamaged cross-section area, considering that carbonation is usually assumed to be

463   associated with the decalcification of the C-A-S-H gel formed during the activation of the slag [20].

464   However, ongoing reduction in the compressive strength with CO_2 exposure is identified in the

465   specimens with GBFS/(GBFS+MK) = 0.8, which were apparently completely carbonated (according

466   to the phenolphthalein test) within the first 250 h of exposure. This highlights the fact that carbonation

467   in alkali-activated binders cannot be understood solely as taking place via either pore solution effects,

468   or by the decalcification of the solid binder phases, but rather that both stages of the interaction

469   between CO_2 and the binder components (liquid and solid) must be considered.

470

471   The chemical reactions controlling the extent of carbonation in alkali-activated materials involve the

472   carbonation of the highly alkaline pore solution, and subsequently carbonation of secondary products

473   such as layered double hydroxides (i.e. hydrotalcite) and decalcification of C-A-S-H type products

474   [22]. Recent work [22] has shown that under accelerated carbonation conditions, the pore solution pH

475   in alkali activated binders is highly dependent on the partial pressure of CO_2, so that a decrease in the

476   pH to values below 10 could only be expected at CO_2 partial pressures higher than ambient, as the

477   pore solution chemistry changes from carbonate-dominated to bicarbonate-dominated. Considering

478   that the phenolphthalein indicator used here shows a colour change at pH values between 8.2 and 10

479   [38], it is likely that the colourless area observed in the carbonation testing is more likely to represent

480   the carbonation of the pore solution, rather than rather than the potential extent of degradation of the

481   C-A-S-H type phases in the binder matrix.

482

483   This is consistent with the fact that the concretes exposed to different CO_2 concentrations present

484   comparable compressive strengths, and that those showing complete carbonation within the first 250 h

485   of exposure report ongoing changes in residual strength after longer times of exposure to CO_2. These

486   later changes in compressive strength are associated with ongoing decalcification processes in the

487   binder, which take place after the local pH has decreased sufficiently to cause phenolphthalein to

488   remain colourless when sprayed onto the samples. It is entirely possible that there is also some

489   decalcification taking place simultaneously at the reaction front where the pH is decreasing, and this

490   will cause the start of the strength loss, but this is seen to continue long after the 'carbonation front'

491   has passed, showing that the traditional conceptual model of this process taking place at a sharp

492   reaction front in Portland cement systems [39] is not appropriate for the systems studied here. It is

493   noted that some authors have also observed a multi-stage process in Portland cement carbonation, e.g.

494   [40], but the details of the mechanisms are likely to be very different in these specimens which do not

495   contain portlandite.

496

497

498   3.2.3.   <u>Water absorption properties</u>

499

500   Given this apparent disconnect between measured carbonation depths and gel decalcification during

501   accelerated carbonation testing of alkali-activated binders, it thus appears valuable to analyse

502   alternative methods by which the progress and effects of the actual decalcification process can be

503   easily determined in an engineering sense, and it is likely that changes in the gel microstructure and

504   pore structure will provide useful information in this regard. Water absorption is a relatively

505   straightforward, although in many cases very sensitive and subtle, means of examining changes in

506   pore network structure. In this section, the effects of inducing carbonation at different CO_2 partial

507   pressures on the water absorption parameters of alkali-activated concretes are assessed.

508

509   •   <u>Volume of permeable pores (ASTM C 642)</u>

510

511   Concretes based solely on GBFS present the lowest volume of permeable pores among the concretes

512   studied prior to carbonation (Figure 6), and an increased volume of pores is identified with the

513   inclusion of higher contents of MK in the binder. This might be an intrinsic property of the more MK-

514   rich binders, but may also be related to the reduced workability identified in these concretes, which

515   makes moulding and compaction of the specimens more difficult. Exposure to 1% CO_2 (Figure 6A)

516   induces a gradual increment in the volume of permeable pores of the specimens throughout the time

517   of exposure, and a very consistent trend in this parameter is observed across the different binder

518   formulations. These results and trends differ from what is usually identified in Portland cement-based

519   materials, where the porosity is generally reduced by carbonation, along with a decrease in the content

520   of small radius pores due to pore blocking by carbonate reaction products [10].

521

522
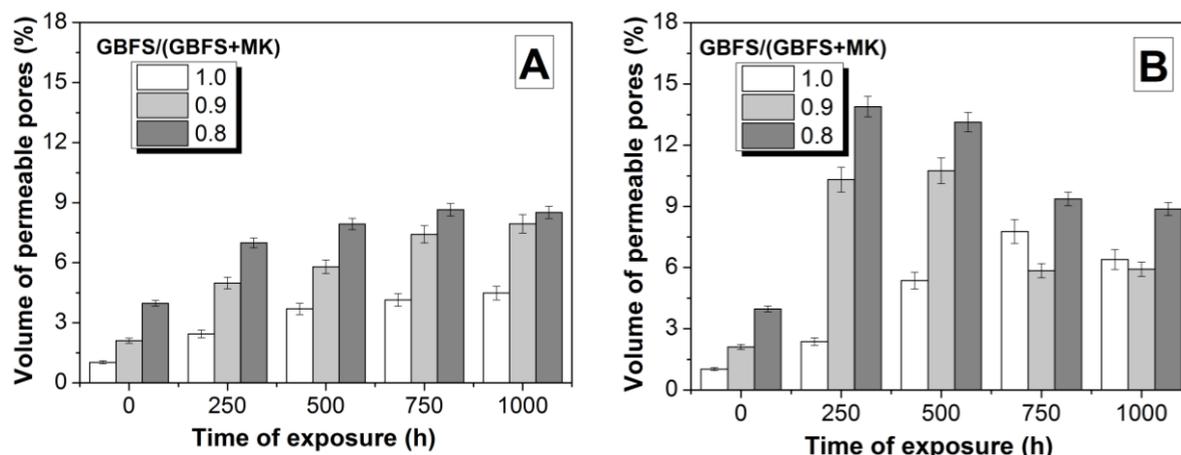
Figure 6. Volume of permeable pores of accelerated carbonated concretes based on alkali-activated slag/metakaolin blends exposed to (A) 1% and (B) 3% CO_2, at 65% RH. Each value is the average of four measurements. Error bars correspond to one standard deviation.

523
524
525

526

527 However, an entirely different trend in the variations of the volume of permeable pores is identified in
528 alkali-activated concretes subjected to accelerated carbonation at 3% CO_2 (Figure 6B). Concretes
529 based solely on GBFS show a gradual increase in porosity during the first 750 h of exposure under
530 these conditions, consistent with the trend identified in these specimens at 1% CO_2 (Figure 6A), but
531 then a decrease in porosity after this time. The concretes with MK in the binder start from a slightly
532 higher porosity, but with exposure to 3% CO_2 show a very substantial increment in their porosity up
533 to 250 h (with GBFS/(GBFS+MK) = 0.8) or 500 h (with GBFS/(GBFS+MK) = 0.9), followed by a
534 significant reduction in porosity up to 1000 h of exposure. These results do not correlate well with the
535 observations related to carbonation front progress or residual compressive strength, where samples
536 with GBFS/(GBFS+MK) = 0.8 were apparently fully carbonated after 250 h of exposure to the same
537 CO_2 concentration, and the variations in strength (Figure 5B) were all monotonic rather than showing
538 any inflection points. It is currently unclear why the samples show a maximum in pore volume after
539 an intermediate duration of carbonation, as this would not logically be expected based on the current
540 understanding of the carbonation mechanisms in these systems, and this issue is identified as being
541 worthy of further analysis as a key part of the future development of reliable carbonation testing
542 protocols for alkali-activated concretes.

543

544 This behaviour provides further evidence that the use of increased concentrations of CO_2 to induce
545 carbonation of alkali-activated concretes leads to unrepresentative, and thus undesirable, changes in
546 the structure and chemistry of alkali-activated binders at early times of CO_2 exposure. This leads to a
547 faster reduction of the pH in the pore solution of the sample, decreasing into the phenolphthalein
548 colour change range, than what would be expected under natural carbonation conditions, and therefore

19

549   the identification of a 'false' carbonation. Consistent with this is the fact that there are ongoing

550   changes in the strength and permeability of 'completely' carbonated specimens, as a consequence of

551   reactions that continue taking place over time. This also agrees with the observation that reductions in

552   the volume of permeable pores are observed here as a consequence of the deposition of solid

553   carbonation products, which appear to contribute to the plugging of some of the additional pores

554   formed during carbonation.

555

556   • Capillary soptivity

557

558   The degradation of reinforced concrete under CO_2 exposure involves both the carbonation of the

559   matrix, leading to a reduction of the alkalinity of the system, and the consequent depassivation of the

560   steel rebars, which makes them susceptible to a series of corrosive attacks such as pitting, which is

561   accelerated by the presence of chloride and is extremely harmful for the integrity of the concrete

562   structure as a whole. It has been reported [41] that similar to the situation for Portland cement based

563   materials, the ingress of chlorine anions into alkali-activated concretes takes place through the

564   capillary pores. Several studies agree [30, 33, 42, 43] that uncarbonated alkali-activated mortars and

565   concretes present low capillary sorptivity, and consequently a high resistance to chloride penetration,

566   when compared with conventional Portland cement concretes; however, the changes in the capillary

567   sorptivity of these concretes induced by carbonation have not previously been studied in detail.

568

569   The exposure to 1% CO_2 of concretes based solely on GBFS (Figure 7A) for 250 h leads to a

570   substantial increment in the total capillary water uptake of the material, which is higher by as much as

571   a factor of 3 than in uncarbonated specimens. However, this dramatic increase is only temporary, and

572   the exposure of these samples to 1% CO_2 for longer periods of times then brings the amount of

573   absorbed water down to be similar to the unexposed material after 750 h of exposure to 1% CO_2. The

574   same is true for the samples with GBFS/(GBFS+MK) = 0.9 (Figure 7B). This indicates that partial

575   carbonation of the specimens may inhibit the ingress of aggressive agents such as chlorides into the

576   concrete, but that the complete carbonation of alkali-activated concretes after this time leads to

577   reductions in the capillarity as a consequence of the precipitation of carbonation products. This time-

578   dependent behaviour was not observed in any other material parameters analysed during exposure to

579   1% CO_2, but shows some subtle effects in changes in pore size distribution which were not observed
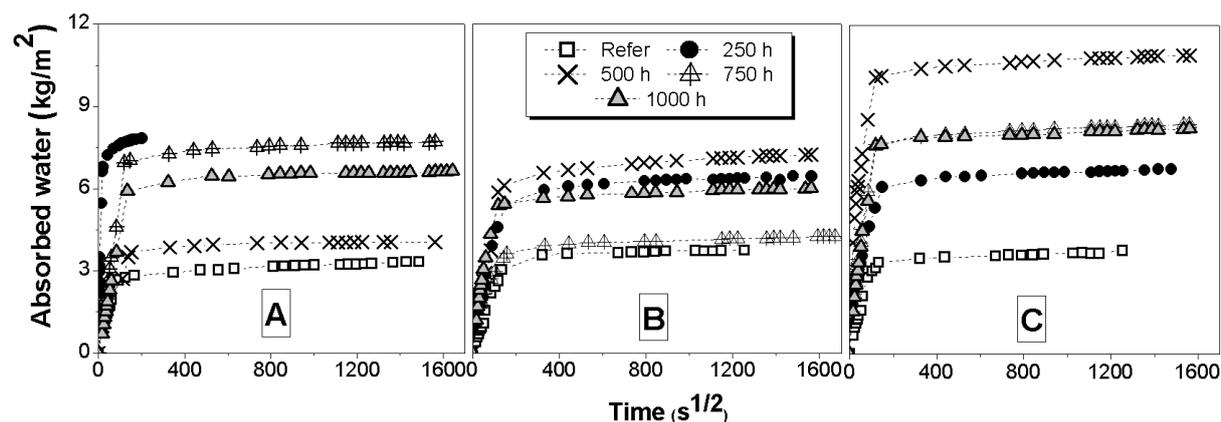
580   in the overall porosity data.

581
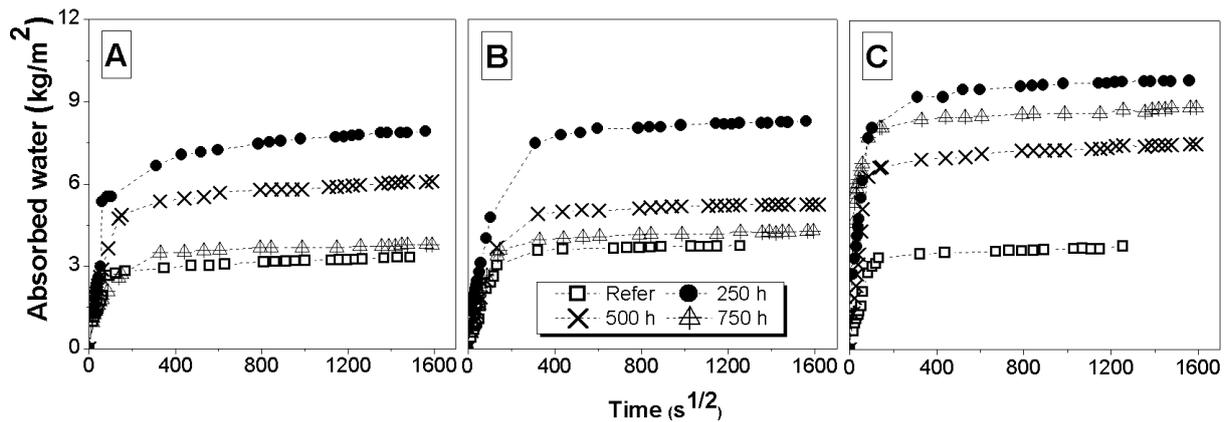
Figure 7. Capillary sorptivity curves of accelerated carbonated concretes based on alkali-activated slag/metakaolin blends formulated with GBFS/(GBFS+MK) ratios of (A) 1.0, (B) 0.9 and (C) 0.8, exposed to 1% CO_2 at 65% RH.

However, concretes formulated with GBFS/(GBFS+MK) = 0.8 (Figure 7C) do not display such a notable reduction in the capillary suction with the progress of carbonation in the specimens. The total water absorbed by the samples exposed to 1% CO_2 for 750 h is almost as high as after 250 h of exposure, and almost three times as high as the water uptake of the unexposed material. This may be associated with the lower Ca content of the gel in this mix, leading to the formation of less solid carbonation products to plug the pores in the material, or may be attributed to factors related to shrinkage and/or microcracking in the gel, which is also likely to be changed by the differences in Ca and Al content as a function of MK addition [29, 30].

Concretes carbonated at a CO_2 concentration of 3% (Figure 8) display water saturation after a shorter period of time than similar concretes carbonated at 1% CO_2 (Figure 7). Concretes exposed to 3% CO_2 for 250 h again show a marked increase in capillary water uptake compared with uncarbonated specimens. After 500 h of exposure (Figure 8A), a substantial reduction in water uptake is identified in specimens based solely on GBFS; however, exposure to this CO_2 concentration for longer periods of time leads again to increments in the amount of absorbed water compared with those identified after 250 h, and the water uptake after 1000 h of carbonation is approximately double the uptake of the unexposed concretes.

21

Figure 8. Capillary sorptivity curves of accelerated carbonated concretes based on activated slag/metakaolin blends formulated with GBFS/(GBFS+MK) ratios of (A) 1.0, (B) 0.9 and (C) 0.8, exposed to 3% CO_2 at 65% RH.

In concretes formulated with GBFS/(GBFS+MK) = 0.9 (Figure 8B), a similar trend is observed, with a reduction in absorbed water after 750 h of exposure but an increased permeability observed at the other times of exposure. This differs from the observations for these concretes when exposed to 1% CO_2, where reductions in the capillary permeability at extended periods of exposure were observed (Figure 7B). This again demonstrates that exposure of alkali-activated concretes to different CO_2 concentrations promotes the development of different pore structures, and therefore variations in the transport of CO_2 inside the material, which can give potentially misleading indications regarding the carbonation performance which would be identified in service in these concretes.

Increasing the MK content of the binder to 20% (GBFS/(GBFS+MK) = 0.8) again leads to increased water absorption at extended times of CO_2 exposure (Figure 8C). This is consistent with the high total porosity observed in these specimens when compared with concretes with lower contents of MK. In this case, similar behaviour is observed at 1% and 3% CO_2 – which may mean either that both of these testing conditions are appropriate for the analysis of these concretes, or that even 1% CO_2 is too high a concentration to provide a good representation of the performance of the concretes in service. At this point it is not possible to say which of these possibilities is more likely, but the effect of elevated CO_2 concentrations on pore solution chemistry [22] indicates that the concentrations are probably too high to fully accurately represent the in-service carbonation of alkali-activated concretes, even at these levels which are quite moderate by the standards of most carbonation tests [28].

The kinetics of the capillary sorption of water into concrete can be described by the resistance to water penetration ($m = \dfrac{\text{saturation time}}{\left(\text{penetration depth}\right)^2}$). The values of this parameter, as determined from

632 capillary sorption curves of concretes exposed to 1% CO_2 (Figure 7) and 3% CO_2 (Figure 8), are

633 shown in Figure 9. Concretes exposed to 1% CO_2 display lower resistance to water penetration at

634 extended periods of exposure, which is consistent with the increased volume of permeable pores

635 observed in those concretes (Figure 6). On the other hand, for concretes exposed to 3% CO_2, the

636 fluctuations in the m values are approximately consistent with the total porosity of these concretes,

637 indicating the high variability of capillary pore structure induced during carbonation at such a high

638 CO_2 concentration.

639
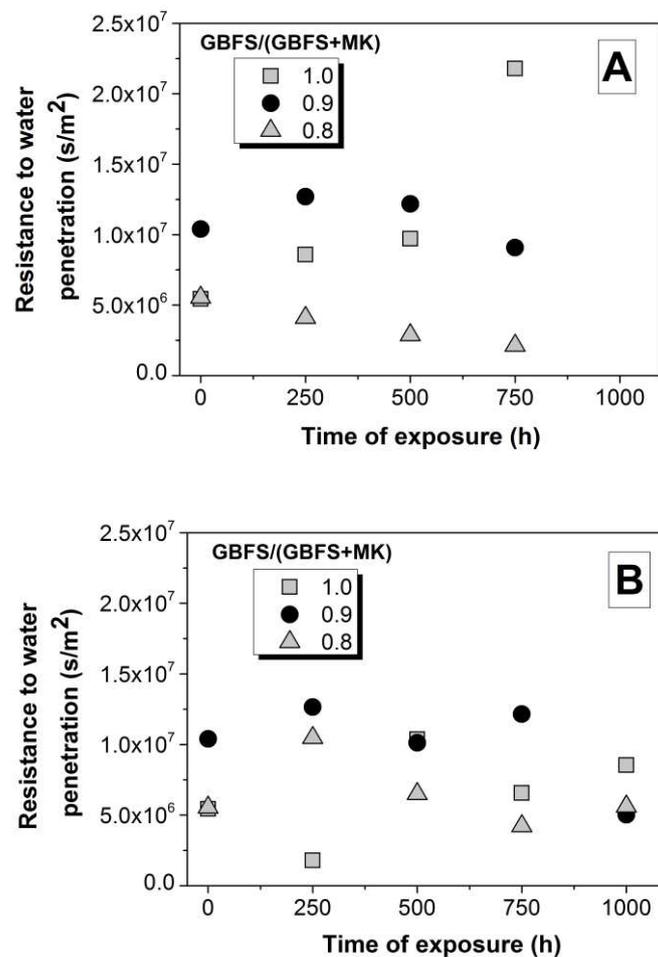
640 **Figure 9.** Resistance to water penetration (m) of carbonated alkali-activated concretes exposed at 65%

641 RH, and (A) 1% CO_2 or (B) 3% CO_2, for durations as marked.

642

643

644

645

646

647

648   **4. Conclusions**

649

650   The key outcome of this study is the observation that accelerated carbonation testing of alkali-
651   activated concretes depends strongly on both the testing conditions and the chemistry of the binder.
652   The inclusion of more than 10% MK (GBFS/(GBFS+MK) < 0.9) in activated-slag binders leads to
653   notably increased carbonation rate and extent, as these specimens develop increased permeability. The
654   performance of samples with GBFS/(GBFS+MK) = 0.9 or 1.0 is sometimes similar, or sometimes the
655   samples with GBFS/(GBFS+MK) = 0.9 carbonate more rapidly, depending on the test conditions. In
656   the relative humidity range tested (50-80%), the highest carbonation rates are generally observed in
657   specimens exposed at a relative humidity of 65±5%, indicating that a partially saturated moisture
658   condition accelerates the carbonation reaction process. For carbonation tests where the specimens
659   were not dried prior to testing, the water absorption of the uncarbonated samples provides a good
660   indication of whether drying effects during the test duration will retard the initial stages of
661   carbonation. Testing samples with low water absorption (i.e. initially highly saturated and refined
662   pore networks) at high relative humidity gives a very low carbonation rate in the early stages of the
663   test, as the carbonation of the saturated binder is slow, followed by an acceleration of the carbonation
664   process as the drying front begins to enter the sample to a more significant extent.

665

666   The progress of carbonation in alkali-activated concretes is also very strongly dependent on the CO_2
667   concentration used during the accelerated testing, as differences in the total porosity and mainly in the
668   capillary pore structure are induced at higher CO_2 concentrations. At relatively low CO_2 concentration
669   (1%), a monotonic increase in porosity, along with an eventual reduction in capillarity, can be
670   identified in the concretes assessed, indicating that the formation of carbonation products in these
671   systems is contributing to changes in the pore network structure during the test. On the other hand,
672   carbonation induced at higher CO_2 concentrations (3%) shows less clarity in the relationships between
673   measured carbonation depth, residual strength and porosity.

674

675   Concretes which appear fully carbonated after only 250 h of testing when the pH is revealed by a
676   phenolphthalein indicator continue to show structural changes over 1000 h, showing that there are
677   likely to be multiple steps in the carbonation process (most probably carbonation of the alkali-rich
678   pore solution in the first instance, followed by later decalcification of the gel), and that the
679   phenolphthalein method shows only the progress of the first of these processes. The rates of pore
680   solution carbonation and gel carbonation seem to be particularly distinct from each other at higher
681   CO_2 concentration, meaning that such test conditions lead to the prediction of poor performance in
682   alkali-activated concretes, which may not accurately represent the behaviour of the materials under
683   exposure to natural carbonation. It is therefore not recommended to carry out accelerated carbonation

684   testing of alkali-activated binders at CO_2 concentrations higher than 1% CO_2. The results obtained

685   from these experiments are more an indication of the loss of alkalinity in these materials due to pore

686   solution chemistry (which is highly subject to differences in CO_2 partial pressure), rather than the

687   degradation due to decalcification of the binding gel, and it cannot be considered as a sole predictor of

688   their durability.

689

690   Finally, it is noted that the interaction between carbonation and drying in alkali-activated concretes

691   certainly requires further investigation – there is a coupling effect whereby drying influences

692   carbonation, and carbonation influences drying, and the study of these effects in parallel in a

693   laboratory (or field) setting has not yet been fully developed. This is an area requiring further

694   research, as highlighted by the fact that this paper has opened almost as many questions as it has

695   answered in this area.

696

697

698   **Acknowledgements**

699

708

709   **References**

710

711   1.   Hobbs DW (2001) Concrete deterioration: causes, diagnosis, and minimising risk. Int
712   Mater Rev 46(3):117-144.
713   2.   Basheer L, Kropp J, Cleland DJ (2001) Assessment of the durability of concrete from
714   its permeation properties: a review. Constr Build Mater 15:93-103.
715   3.   Poonguzhali A, Shaikh H, Dayal RK, Khatak HS (2008) Degradation mechanism and
716   life estimation of civil structures – A review. Corros Rev 26(4):215-294.
717   4.   Fernández-Bertos M, Simons SJR, Hills CD, Carey PJ (2004) A review of accelerated
718   carbonation technology in the treatment of cement-based materials and sequestration
719   of CO_2. J Hazard Mater B112:193-205.
720   5.   Bary B, Sellier A (2001) Coupled moisture—carbon dioxide–calcium transfer model
721   for carbonation of concrete. Cem Concr Res 34:1859-1872.

722 6. Živica V, Bajza A (2001) Acidic attack of cement based materials — a review: Part 1.
723   Principle of acidic attack. Constr Build Mater 15(8):331-340.
724 7. Johannesson B, Utgenannt P (2001) Microstructural changes caused by carbonation of
725   cement mortar. Cem Concr Res 31:925-931.
726 8. Papadakis VG, Vayenas CG, Fardis MN (1989) A reaction engineering approach to
727   the problem of concrete carbonation. AIChE J 35(10):1639-1650.
728 9. Papadakis VG, Vayenas CG, Fardis MN (1991) Experimental investigation and
729   mathematical modeling of the concrete carbonation problem. Chem Eng Sci 46:1333-
730   1338.
731 10. Houst YF, Wittmann FH (1994) Influence of porosity and water content on the
732   diffusivity of CO_2 and O_2 through hydrated cement paste. Cem. Concr. Res.
733   24(6):1165 - 1176.
734 11. Houst YF (1996) The role of moisture in the carbonation of cementitious materials.
735   Int. Z. Bauinst. 2(1):49 - 66.
736 12. Younsi A, Turcry P, Aït-Mokhtar A, Staquet S (2013) Accelerated carbonation of
737   concrete with high content of mineral additions: Effect of interactions between
738   hydration and drying. Cem Concr Res 43:25-33.
739 13. Deja J (2002) Carbonation aspects of alkali activated slag mortars and concretes. Silic
740   Industr 67(1):37-42.
741 14. Shi C, Krivenko PV, Roy DM. Alkali-Activated Cements and Concretes, Abingdon,
742   UK: Taylor & Francis, 2006.
743 15. Xu H, Provis JL, van Deventer JSJ, Krivenko PV (2008) Characterization of aged slag
744   concretes. ACI Mater J 105(2):131-139.
745 16. Bernal SA, San Nicolas R, Provis JL, Mejía de Gutiérrez R, van Deventer JSJ (2014)
746   Natural carbonation of aged alkali-activated slag concretes. Mater Struct DOI:
747   10.1617/s11527-013-0089-2.
748 17. Bernal SA, Mejía de Gutierrez R, Rose V, Provis JL (2010) Effect of silicate modulus
749   and metakaolin incorporation on the carbonation of alkali silicate-activated slags.
750   Cem Concr Res 40(6):898-907.
751 18. Puertas F, Palacios M, Vázquez T (2006) Carbonation process of alkali-activated slag
752   mortars. J Mater Sci 41:3071-3082.
753 19. Palacios M, Puertas F (2006) Effect of carbonation on alkali-activated slag paste. J
754   Am Ceram Soc 89(10):3211-3221.
755 20. Bernal SA, Provis JL, Walkley B, San Nicolas R, Gehman JD, Brice DG, Kilcullen A,
756   Duxson P, van Deventer JSJ (2013) Gel nanostructure in alkali-activated binders
757   based on slag and fly ash, and effects of accelerated carbonation. Cem Concr Res
758   53:127-144.
759 21. Bernal SA, San Nicolas R, Myers RJ, Mejía de Gutiérrez R, Puertas F, van Deventer
760   JSJ, Provis JL (2014) MgO content of slag controls phase evolution and structural
761   changes induced by accelerated carbonation in alkali-activated binders. Cem Concr
762   Res 57:33-43.
763 22. Bernal SA, Provis JL, Brice DG, Kilcullen A, Duxson P, van Deventer JSJ (2012)
764   Accelerated carbonation testing of alkali-activated binders significantly underestimate
765   the real service life: The role of the pore solution. Cem Concr Res 42(10):1317-1326.
766 23. Ismail I, Bernal SA, Provis JL, Hamdan S, van Deventer JSJ (2013) Drying-induced
767   changes in the structure of alkali-activated pastes. J Mater Sci 48:3566-3577.
768 24. Ishida T, Meakawa K, Soltani M (2004) Theoretically identified strong coupling of
769   carbonation rate and thermodynamic moisture states in micropores of concrete.
770   2(2):213 - 222.

25. EN 13295:2004: Products and systems for the protection and repair of concrete structures – test methods – Determination of resistance to carbonation. .

26. Harrison TA, Jones MR, Newlands MD, Kandasami S, Khanna G (2012) Experience of using the prTS 12390-12 accelerated carbonation test to assess the relative performance of concrete. Mag Concr Res 64(8):737-747.

27. Sanjuán MA, Andrade C, Cheyrezy M (2003) Concrete carbonation test in natural and accelerated conditions. Adv Cem Res 15(4):171 - 180.

28. da Silva FG, Helene P, Castro-Borges P, Liborio JBL (2009) Sources of variations when comparing concrete carbonation results. J Mater Civ Eng 21(7):333-342.

29. Bernal SA, Provis JL, Mejía de Gutierrez R, Rose V (2011) Evolution of binder structure in sodium silicate-activated slag-metakaolin blends. Cem Concr Compos 33(1):46-54.

30. Bernal SA, Mejía de Gutierrez R, Provis JL (2012) Engineering and durability properties of concretes based on alkali-activated granulated blast furnace slag/metakaolin blends. Constr Build Mater 33:99-108.

31. Fagerlund G (1982) On the capillarity of concrete. Nord Concr Res 1:6.1-6.20.

32. Levenspiel O. Chemical Reaction Engineering, 3rd Ed., New York: Wiley, 1999.

33. Bernal SA, Mejía de Gutierrez R, Pedraza AL, Provis JL, Rodríguez ED, Delvasto S (2011) Effect of binder content on the performance of alkali-activated slag concretes. Cem Concr Res 41(1):1-8.

34. Roy SK, Poh KB, Northwood DO (1999) Durability of concrete—accelerated carbonation and weathering studies. Build. Environ. 34(5):597-606.

35. El-Turki A, Ball RJ, Allen GC (2007) The influence of relative humidity on structural and chemical changes during carbonation of hydraulic lime. Cem. Concr. Res. 37(8):1233-1240.

36. Collins F, Sanjayan JG (2000) Effect of pore size distribution on drying shrinking of alkali-activated slag concrete. Cem Concr Res 30(9):1401-1406.

37. Hyvert N, Sellier A, Duprat F, Rougeau P, Francisco P (2010) Dependency of C–S–H carbonation rate on CO_2 pressure to explain transition from accelerated tests to natural carbonation. Cem Concr Res 40(11):1582-1589.

38. Vassie PR. Measurement techniques for the diagnosis, detection and rate estimation of corrosion in concrete structures. In: Dhir RK, Newlands MD, eds. Controlling concrete degradation, Proceedings of the International Seminar. Dundee, Scotland, Thomas Telford, 1999. pp. 215-229.

39. Castellote M, Andrade C (2008) Modelling the carbonation of cementitious matrixes by means of the unreacted-core model, UR-CORE. Cem Concr Res 38(12):1374-1384.

40. Thiery M, Villain G, Dangla P, Platret G (2007) Investigation of the carbonation front shape on cementitious materials: Effects of the chemical kinetics. Cem Concr Res 37(7):1047-1058.

41. Roy DM, Jiang W, Silsbee MR (2000) Chloride diffusion in ordinary, blended, and alkali-activated cement pastes and its relation to other properties. Cem Concr Res 30:1879-1884.

42. Collins F, Sanjayan J (2010) Capillary shape: Influence on water transport within unsaturated alkali activated slag concrete. J Mater Civil Eng 22(3):260-266.

43. Shi C (1996) Strength, pore structure and permeability of alkali-activated slag mortars. Cem Concr Res 26(12):1789-1799.